Supporting Information

Balancing Solvation: Stabilizing Lithium Metal Batteries via Optimized Cosolvents in Ionic-liquid Electrolytes

Xinlin Li,[a] Xianyang Wu,[a] Seoung-Bum Son,[a] Jorge Seminario,[b, d, e*] Perla Balbuena,[b, e, f*] Anderson Arboleda,[b] Jiyu Cai,[a] Matthew Li,[a] Ziyuan Lyu,[g,h] Dominic Bresser,[g,h] Rachid Amine,[c] Chi-Cheung Su,[a*] and Khalil Amine[a*]

[a] Chemical Sciences and Engineering Division, Argonne National Laboratory, 9700 S. Cass Avenue, Lemont, IL 60439, USA

[b] Department of Chemical Engineering, Texas A&M University, College Station, Texas, 77843, USA

[c] Materials Science Division, Argonne National Laboratory, 9700 S. Cass Avenue, Lemont, IL 60439, USA

[d] Department of Electrical and Computer Engineering, Texas A&M University, College Station, Texas, 77843, USA

[e] Department of Materials Science and Engineering, Texas A&M University, College Station, Texas, 77843, USA

[f] Department of Chemistry, Texas A&M University, College Station, Texas, 77843, USA

[g] Helmholtz Institute Ulm (HIU), Electrochemical Energy Storage, 89081 Ulm, Germany

[h] Karlsruhe Institute of Technology (KIT), 76021 Karlsruhe, Germany

E-mail: csu@anl.gov; seminario@tamu.edu; balbuena@tamu.edu; amine@anl.gov

Experimental Section

Electrode Materials: Cathode NMC811 ($LiNi_{0.8}Mn_{0.1}Co_{0.1}O_2$) was supplied by the Cell Analysis, Modeling, and Prototyping (CAMP) Facility at Argonne National Laboratory. The composition of NMC811 cathode is 90 wt.% NMC811, 5 wt.% carbon black, and 5 wt.% PVDF binder calendared to 36.3% porosity with 8.34 mg/cm^2 active material loading. The NMC811 laminates were punched into 14-mm discs and the punched discs were dried at 100°C under vacuum overnight.

Cell Assembly: A 2032 type coin cell was used for battery testing and all cells were prepared in an argon-atmosphere glovebox (<1 ppm of O_2 and H_2O. A coated PP separator with an effective diameter of 16 mm was used. Lithium disks with a diameter of 16 mm were used as received as both the counter and reference electrodes. For Li||Cu cells, the Cu foil used for cathode was treated by soaking in 1M H_2SO_4 for 4 days to remove CuO on the surface, followed by washing with ethanol and acetone. The effective area of the Cu foil for Li deposition was 0.97 cm^2. 30 μL of prepared electrolytes were used in all cells.

Electrolytes materials & preparation: The ionic liquid, N-Methyl-N-Propylpyrrolidinium Bis(fluorosulfonyl)imide (Py1,3 FSI), was purchased from TCI America and dried with 4-Å molecular sieves before use. 1,1,1-trifluoro-2-(2-(2-(2,2,2-trifluoroethoxy)ethoxy)ethoxy)ethane (FDG) was synthesized according to a reported procedure.[1] The cosolvents, diglyme (DG), and 1, 1, 2, 2-Tetrafluoroethyl-2, 2, 3, 3-tetrafluoropropyl ether (TTE) were dried with 4-Å molecular sieves before use. Battery-grade Lithium bis(fluorosulfonyl)imide (LiFSI) was purchased from BASF and used as received. All electrolyte solutions were prepared in an argon-atmosphere glovebox with O_2 and H_2O level below 1 ppm. LiFSI was dissolved in mixed solvents in desired volume ratio and was stirred until completely dissolved.

Electrochemical tests: Galvanostatic charge/discharge cycling was performed on MACCOR Electrochemical Analyzer. For Li||NMC811 cells, three formation cycles were carried out at a rate of C/10 which was followed by a rate of C/2, with a voltage cutoff between 4.3 and 3.0 V.

For the Li||Cu Coulombic efficiency tests, 4 mAh cm^{-2} of lithium metal was deposited on the Cu foil at 0.1 mA cm^{-2} current density, and then plating and stripping were performed at 1 mA cm^{-2} for 9 cycles before stripping all the lithium at 0.1 mA cm^{-2} until the cell potential reached 1 V. The effective area of the Cu foil for Li deposition was 0.97 cm^2. Li||Li symmetric cells were tested through a galvanostatic charge and discharge protocol at the current density of 1mA cm^{-2}., Each charge and discharge process lasts for 90 min. The electrochemical impedance spectra were collected using a Solartron electrochemical working station operated between 0.01 Hz and 1 MHz with the amplitude of 10 mV. The transference number of electrolytes were measured via a direct polarization method with a polarization bias of 30mV on a Solartron electrochemical working station. The transference number (t_{Li^+})is calculated using equation below:

$$t_{Li+} = \frac{I_{SS}(\Delta V - I_0 R_0)}{I_0(\Delta V - I_{SS} R_{SS})}$$

Electrolyte characterization: Conductivity was measured by an AC impedance technique using a coin cell fixture. The impedance spectra were obtained on Gamry Interface 5000 in the frequency range of 0.01 Hz to 1MHz under a potential of 10 mV. A coin cell fixture containing 170 µL of targeted electrolyte was placed in the oven with programed temperature control.

FTIR spectra were acquired in the attenuated total reflection mode with 2 cm^{-1} resolution with one scan to avoid evaporation of the volatile solvents.

The viscosity of electrolytes were collected on ViscoLab 4000 manufactured by Cambridge Viscosity which was equipped with a water circulator to maintain desired temperature.

DFT calculation Methods: DFT calculations for HOMO and LUMO energies and molecular electrostatic potentials (MEP) of solvent molecules were performed using the B3LYP/6-31+G(d,p) level of theory on Gaussian 16.[2] Visualization of molecular orbitals and analysis of MEP were conducted on Gauss view, Multiwfn[3] and Visual Molecular Dynamics (VMD)[4] software. The implicit Solvation Model on Density (SMD) was applied to simulate the effect of solvents on molecules but then the explicit solvent was included.

Molecular Dynamics Simulation Methods: We used the program LAMMPS with the ReaXX force field. Before doing the molecular dynamics simulations, we performed a full optimization of the geometry of the samples. Then, we performed an equilibration at 5K using sequentially the ensembles NVT, NPT and then back to NVT. This equilibrations were followed by a linear heating from 5K to 330K using the NPT emsemble. Finally the sample was equilibrated at 330K, following the same protocol used at 5K.

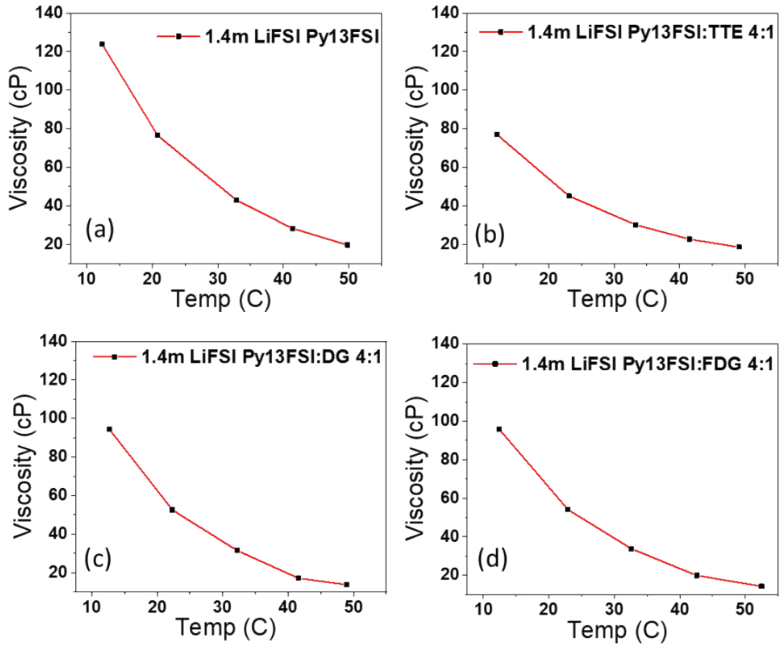

Figure S1. Temperature dependent viscosity of tested electrolytes. Detailed compositions are described in the legend of each panel.

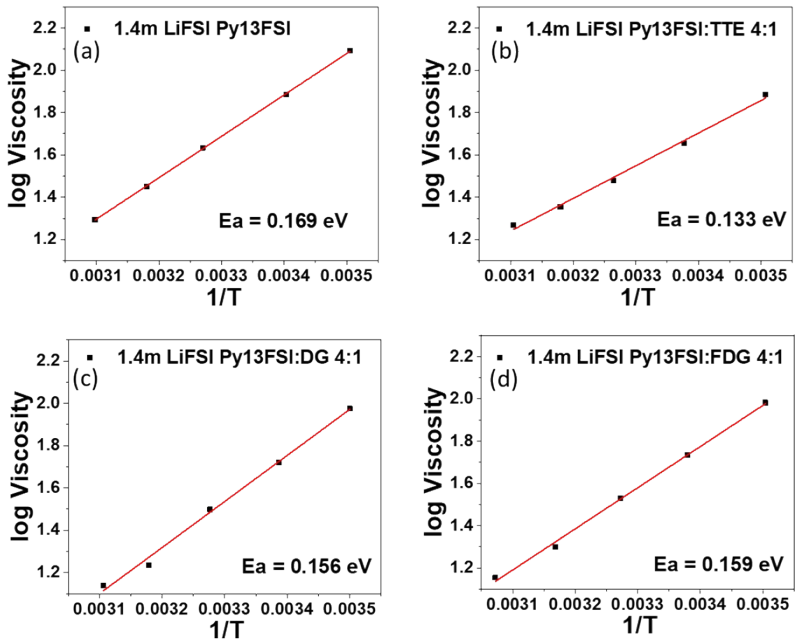

Figure S2. Viscosity activation energy of tested electrolytes calculated from temperature dependent viscosity measurements. Detailed compositions are described in the legend of each panel.

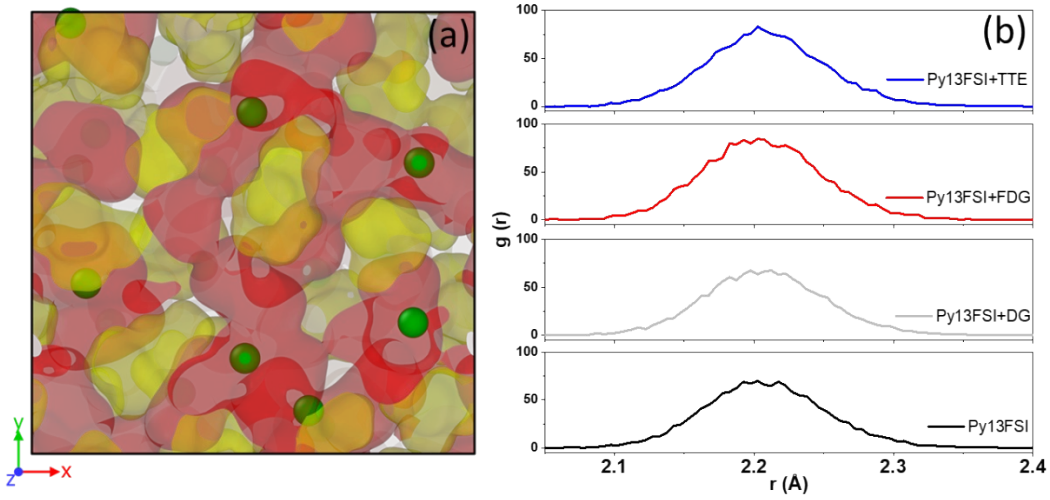

Figure S3. (a) Snapshot of MD simulation box for Py13FSI electrolyte. Green spheres, red, and yellow clouds stand for Li ions, FSI anions, and Py13 cations. (b) radial distribution of Li-O_{FSI} in four electrolytes.

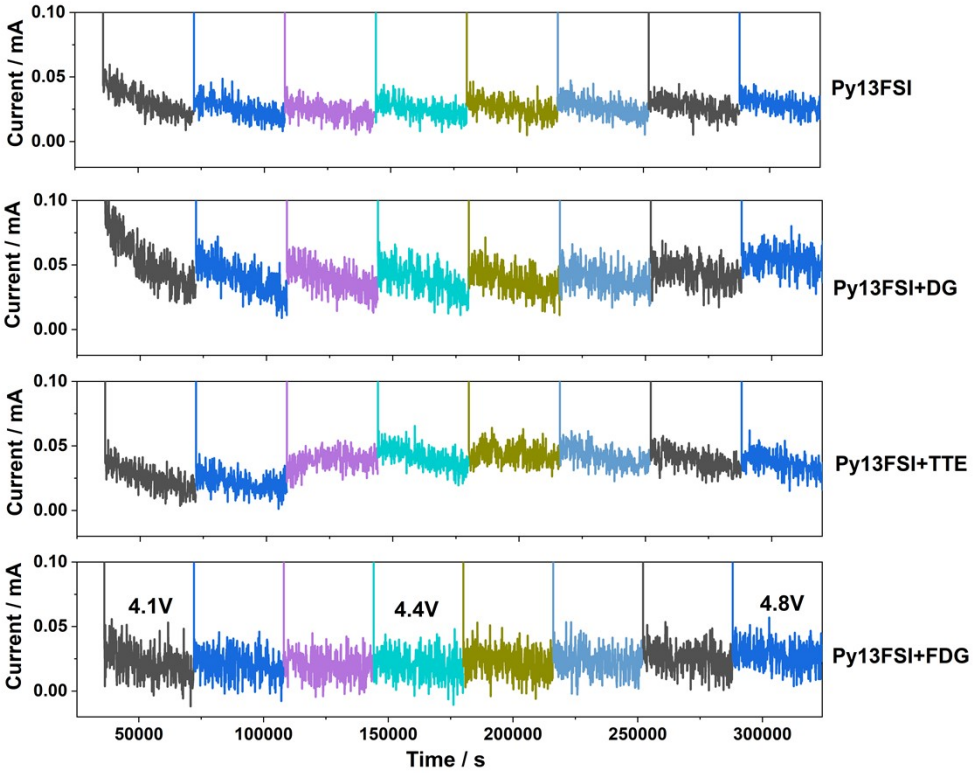

Figure S4. Chronoamperograms of Li||Al cells with electrolytes containing different cosolvents with a step potential of 0.1 V (4.1-4.8 V) and a holding time of 30 h for each potential.

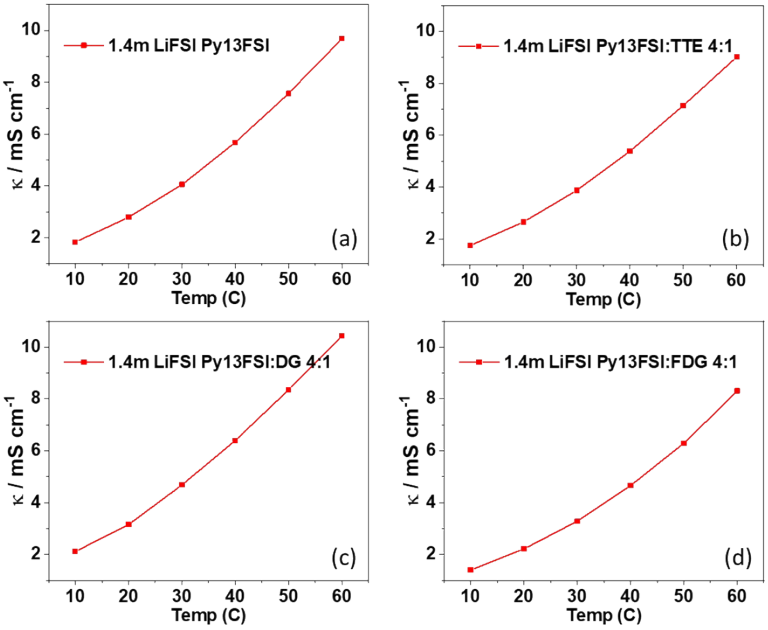

Figure S5. Temperature dependent conductivity of tested electrolytes. Detailed compositions are described in the legend of each panel.

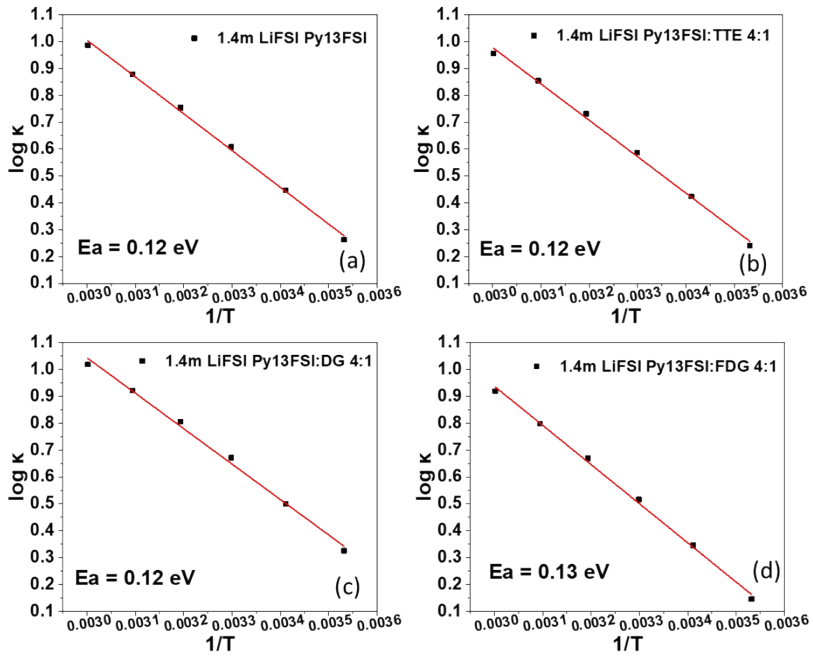

Figure S6. Conductivity activation energy of tested electrolytes calculated from temperature dependent viscosity measurements. Detailed compositions are described in the legend of each panel.

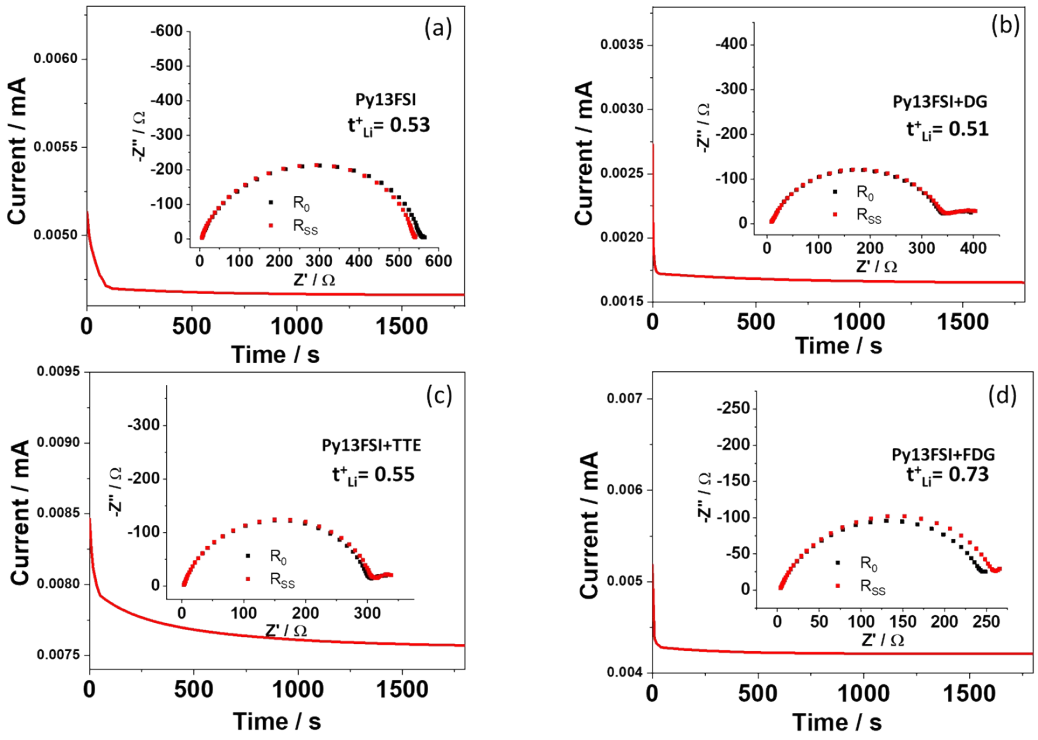

Figure S7. Chronoamperograms and Nyquist plots (insets) of Li||Li cells with (a) Py13FSI, (b) Py13FSI+DG, (c) Py13FSI+TTE, (d) Py13FSI+FDG electrolytes.

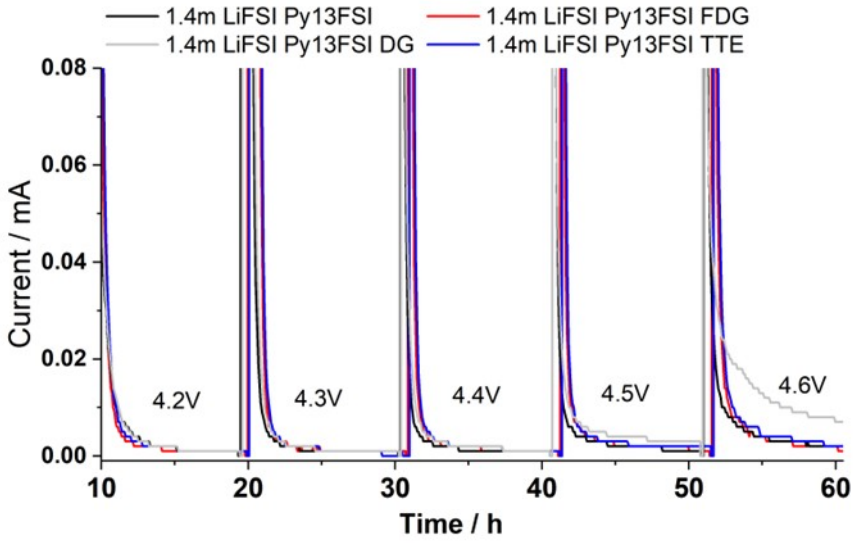

Figure S8. Chronoamperograms of Li||NMC811 cells with different electrolytes with a step potential of 0.1 V (4.2-4.6 V) and a holding time of 10 h for each potential. The leakage current reflects the extent of side reactions at each potential.

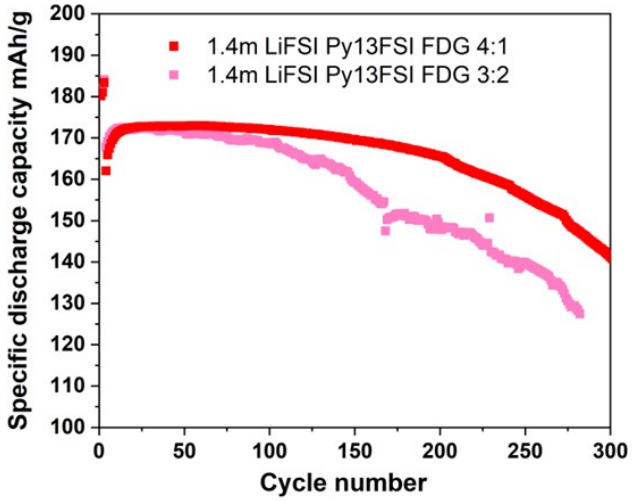

Figure S9. Cycling test results of electrolytes with different volumetric ratio of cosolvents. Tests were conducted in Li||NMC811 cells with a cutoff voltage of 3.0-4.3V at a rate of C/3.

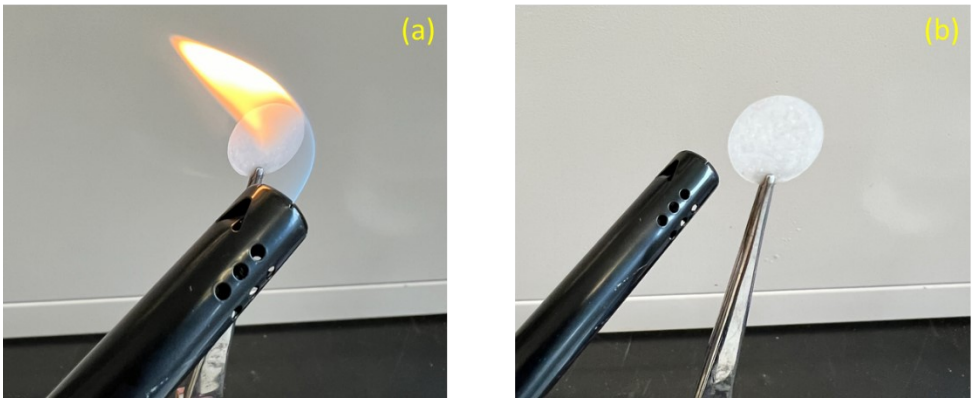

Figure S10. Ignition experiment showing fire-retardant feature of the Py13FSI+FDG electrolyte. Panel (a) and (b) display the photo of electrolyte-soaked glass fiber with flame on and off, respectively. The observation demonstrates the fire-retardant property of this ionic-liquid-based electrolyte.

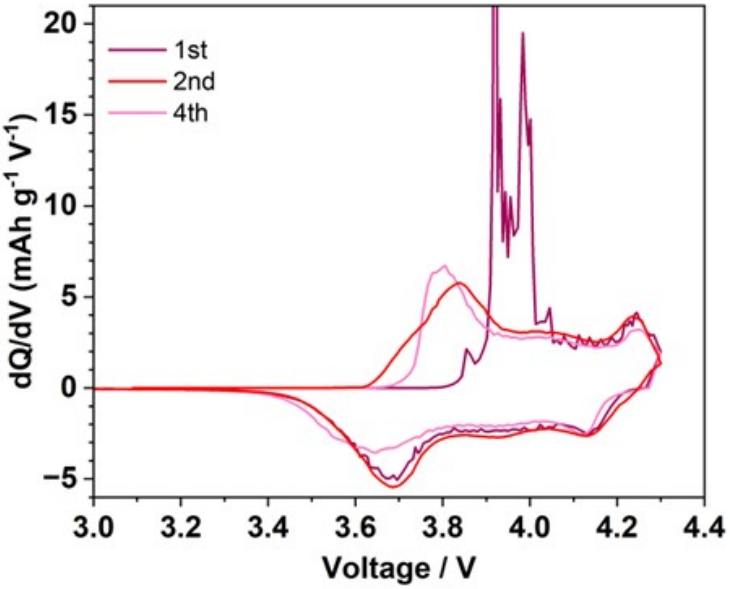

Figure S11. Differential capacity curves at selected cycles in Li||NMC811 cells with Py13FSI:FDG 4:1 electrolyte.

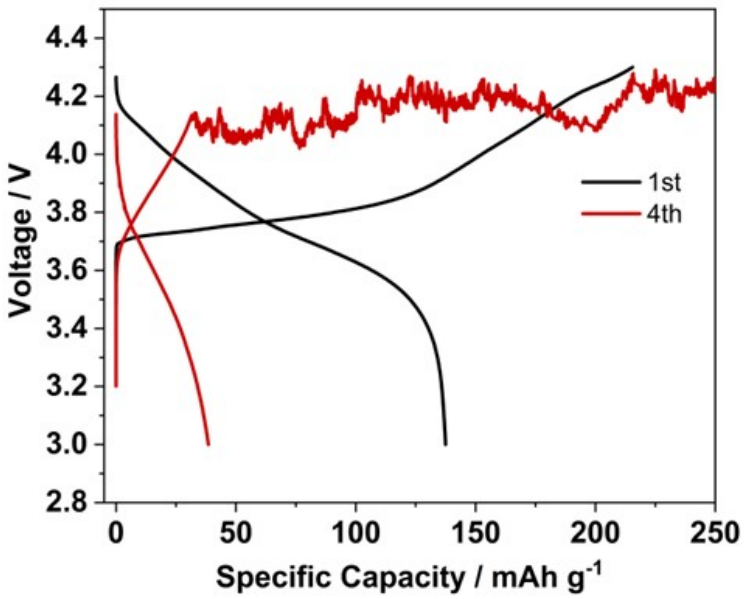

Figure S12. Selected voltage-capacity curves of Li||NMC811 cells filled with Py13FSI+DG electrolyte.

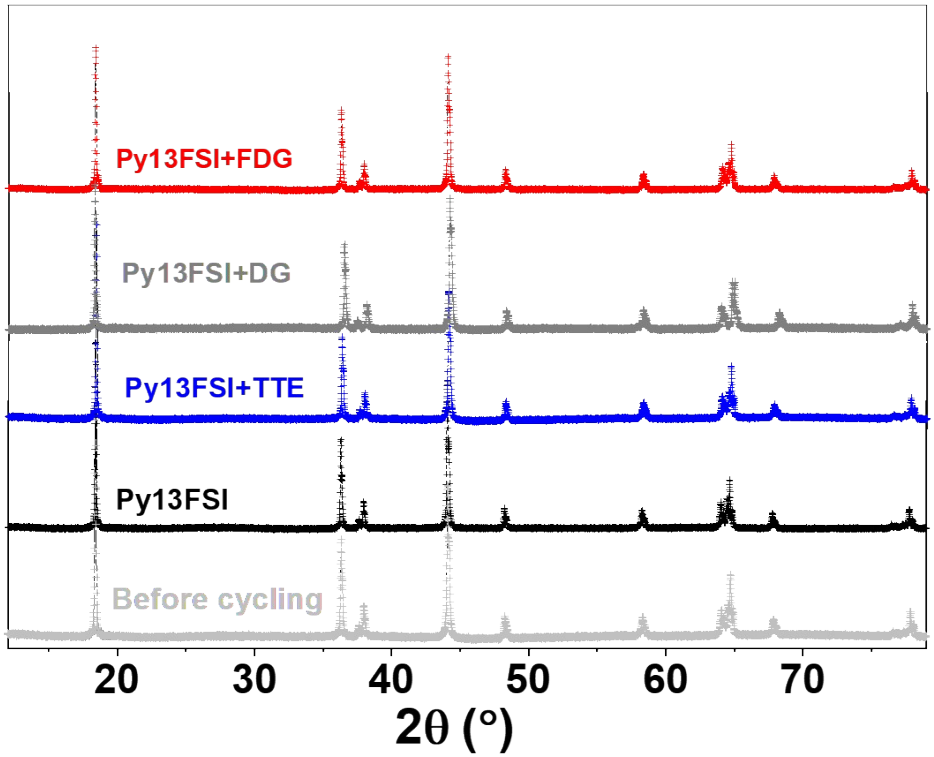

Figure S13. XRD patterns of NMC811 cathodes dissembled from cells with different electrolytes after cycling.

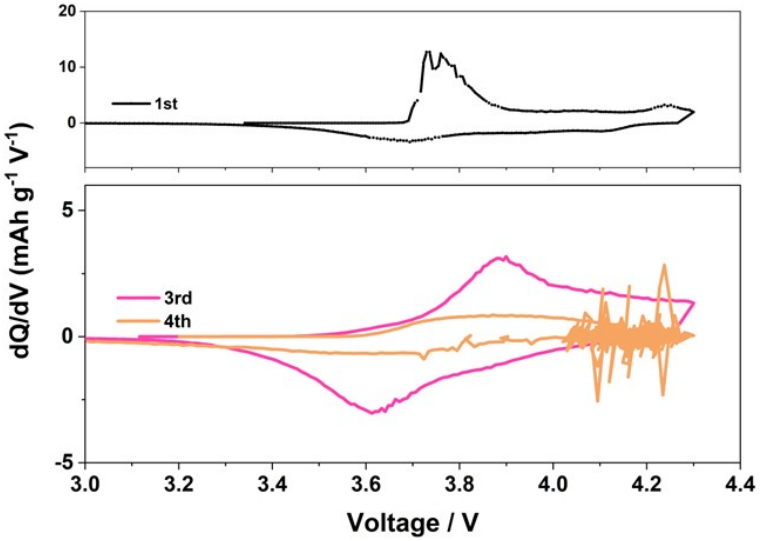

Figure S14. Differential capacity curves at selected cycles in Li||NMC811 cells filled with Py13FSI+DG electrolyte.

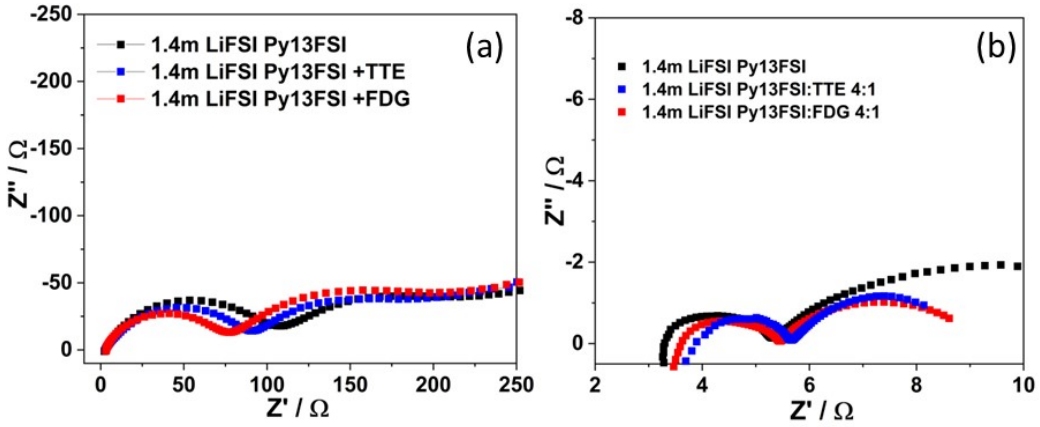

Figure S15. Nyquist plots of EIS collected from (a) Li||NMC cells with varied electrolytes after formation cycles (b) Li||Li cells charge and discharged for 30 h (15 cycles) under a current density of 1mA/cm^2.

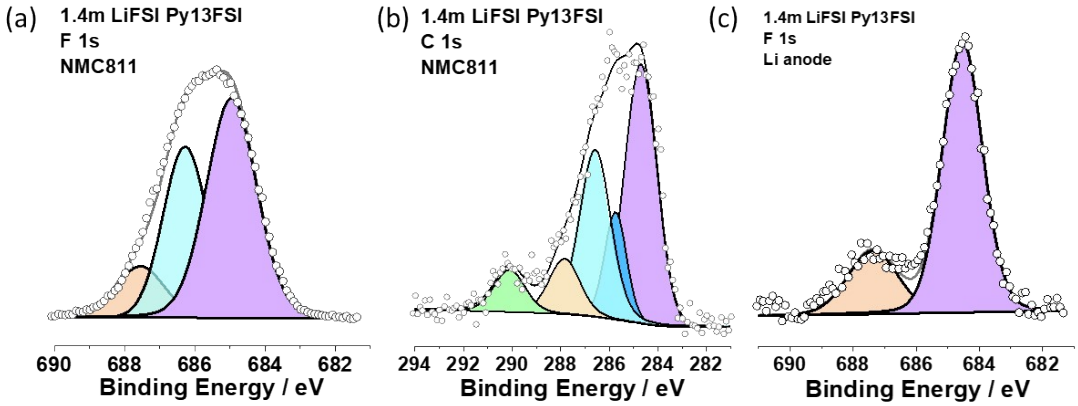

Figure S16. XPS spectra of (a) F1s and (b) C1s collected from NMC811 cathode, (c) F1s collected from Li anode. Electrodes were dissembled from cycled cells with Py13FSI electrolyte.

Table S1. Summary of cycling data of Li||NMC811 cell operated at voltage range of 3.0–4.3 V with ionic-liquid electrolytes with different cosolvents: 1st-cycle Coulombic efficiency (1st CE), 1st-cycle discharge capacity (1st DC), Cycle number on 80% capacity retention (CN-80), and average CE of 100 cycles (100-ACE).

Electrolyte	Composition	1st CE	1st DC (mAh/g)	Cycle number on 80% capacity retention (CN-70)	100-ACE
E1	1.4m LiFSI Py13FSI	82.87%	183.3	83	99.48
E2	1.4m LiFSI Py13FSI:TTE 4:1 (V/V)	83.84%	189.0	171	99.71
E3	1.4m LiFSI Py13FSI:DG 4:1(V:V)	68.74%	157.3	<3	- -
E4	1.4m LiFSI Py13FSI:FDG 4:1 (V/V)	82.07%	181.2	320	99.74

Table S2. Summary of species and corresponding binding energies, relative quantities obtained from XPS data collected from cycled cells with tested electrolytes.

Electrolyte		Element	Binding energy	Species	%Area
1.4m LiFSI Py13FSI	Cathode	C1s	284.7	C-C	43.1
			285.7	C-O	12.3
			286.6	C-N	28.1
			287.8	C=O	9.3
			290.1	$(CO_3)^{2-}$	7.2
		F1s	685.0	LiF	53.4
			686.3	C-F	34.7
			687.6	SO_2-F	11.9
1.4m LiFSI Py13FSI:TTE 4:1		C1s	284.7	C-C	37.9
			285.7	C-O	13.1
			286.6	C-N	32.0
			287.8	C=O	11.3
			290.1	$(CO_3)^{2-}$	5.7
		F1s	684.9	LiF	46.2
			686.3	C-F	38.0
			687.6	SO_2-F	15.8
1.4m LiFSI Py13FSI:FDG 4:1		C1s	284.9	C-C	34.1
			285.7	C-O	8.1
			286.6	C-N	31.7
			287.8	C=O	15.7
			290.1	$(CO_3)^{2-}$	4.3
			291.1	CF_3	6.1
		F1s	685.1	LiF	26.2
			686.3	C-F	36.3
			687.6	SO_2-F	37.5
1.4m LiFSI Py13FSI	Anode	F1s	684.5	LiF	77.5
			687.4	SO_2-F	22.5
1.4m LiFSI Py13FSI:TTE 4:1		F1s	684.7	LiF	83.7
			687.6	SO_2-F	16.3
1.4m LiFSI Py13FSI:FDG 4:1		F1s	684.7	LiF	75.8
			687.6	SO_2-F	24.2

References:

1. Su, C.-C.; Shi, J.; Amine, R.; He, M.; Son, S.-B.; Guo, J.; Jiang, M.; Amine, K., Terminally fluorinated glycol ether electrolyte for lithium metal batteries. *Nano Energy* **2023,** *110*, 108335.
2. M. J. Frisch; G. W. Trucks; H. B. Schlegel; G. E. Scuseria; M. A. Robb; J. R. Cheeseman; G. Scalmani; V. Barone; B. Mennucci; G. A. Petersson; H. Nakatsuji; M. Caricato; X. Li; H. P. Hratchian; A. F. Izmaylov; J. Bloino, G. Z.; J. L. Sonnenberg; M. Hada; M. Ehara; K.Toyota; R. Fukuda; J. Hasegawa; M. Ishida; T. Nakajima; Y. Honda; O. Kitao; H. Nakai; T. Vreven; J. A. Montgomery; Jr., J. E. P.; F. Ogliaro; M. Bearpark; J. J. Heyd; E. Brothers; K. N. Kudin; V. N. Staroverov; T. Keith; R. Kobayashi; J. Normand; K. Raghavachari; A. Rendell; J. C. Burant; S. S. Iyengar; J. Tomasi; M. Cossi; N. Rega; J. M. Millam; M. Klene; J. E. Knox; J. B. Cross; V. Bakken; C. Adamo; J. Jaramillo; R. Gomperts; R. E. Stratmann; O. Yazyev; A. J. Austin; R. Cammi; C. Pomelli; J. W. Ochterski; R. L. Martin; K. Morokuma; V. G. Zakrzewski; G. A. Voth; P. Salvador; J. J. Dannenberg; S. Dapprich; A. D. Daniels; O. Farkas; J. B. Foresman; J. V. Ortiz; J. Cioslowski; Fox, D. J., Gaussian 09, Revision D.01,. *Gaussian, Inc., Wallingford CT,* **2013**.
3. Lu, T.; Chen, F., Multiwfn: A multifunctional wavefunction analyzer. *J. Comput. Chem.* **2012,** *33* (5), 580-592.
4. Humphrey, W.; Dalke, A.; Schulten, K., VMD: Visual molecular dynamics. *Journal of Molecular Graphics* **1996,** *14* (1), 33-38.